

## A covariation analysis reveals elements of selectivity in quorum sensing systems

Wellington Miranda, S<sup>1</sup>, Cong, Q<sup>2,3,4,5</sup>, Schaefer, AL<sup>1</sup>, MacLeod, EK<sup>1</sup>, Zimenko, A<sup>1</sup>, Baker, D<sup>2,3,6</sup>, & Greenberg, EP<sup>1,\*</sup>

1. Department of Microbiology, University of Washington, Seattle, WA 98195, USA
2. Department of Biochemistry, University of Washington, Seattle, WA 98105, USA
3. Institute for Protein Design, University of Washington, Seattle, WA 98105, USA
4. Eugene McDermott Center for Human Growth and Development, University of Texas Southwestern Medical Center, Dallas, Texas 75390, USA
5. Department of Biophysics, University of Texas Southwestern Medical Center, Dallas, TX 75390, USA
6. Howard Hughes Medical Institute, University of Washington, Seattle, WA 98105, USA

\*Corresponding author, [epgreen@uw.edu](mailto:epgreen@uw.edu)

## Abstract

1 Many bacteria communicate with kin and coordinate group behaviors through a form of cell-cell  
2 signaling called acyl-homoserine lactone (AHL) quorum sensing (QS). In these systems, a signal  
3 synthase produces an AHL to which its paired receptor selectively responds. Selectivity is fundamental  
4 to cell signaling. Despite its importance, it has been challenging to determine how this selectivity is  
5 achieved and how AHL QS systems evolve and diversify. We hypothesized that we could use  
6 covariation within the protein sequences of AHL synthases and receptors to identify selectivity residues.  
7 We began by identifying about 6,000 unique synthase-receptor pairs. We then used the protein  
8 sequences of these pairs to identify covariation patterns and mapped the patterns onto the LasI/R system  
9 from *Pseudomonas aeruginosa* PAO1. The covarying residues in both proteins cluster around the ligand  
10 binding sites. We demonstrate that these residues are involved in system selectivity toward the cognate  
11 signal and go on to engineer the Las system to both produce and respond to an alternate AHL signal. We  
12 have thus demonstrated a new application for covariation methods and have deepened our understanding  
13 of how communication systems evolve and diversify.

14 Quorum sensing (QS) is a widespread form of cell-cell signaling that bacteria use to coordinate  
15 the production of public goods including toxins, antibiotics, bioluminescence, and secreted enzymes<sup>1,2</sup>.  
16 Many Proteobacteria<sup>3</sup> and Nitrospirae<sup>4</sup> employ a form of QS based on acyl-homoserine lactone (AHL)  
17 signals. AHL QS systems consist of two proteins: a LuxI-type signal synthase and a LuxR-type receptor  
18 (Figure 1a). The signal synthase produces an AHL from S-adenosylmethionine (SAM) and an acyl-acyl  
19 carrier protein (ACP) for some LuxI-type synthases or an acyl-coenzyme A (CoA) substrate for others<sup>5</sup>  
20 (Fig. 1b). AHL signals can freely diffuse through cell membranes<sup>6,7</sup> and at low cell density the QS  
21 system is “off”. At high cell density, the signal accumulates and binds the LuxR-type receptor which is a  
22 cytosolic transcription factor that regulates gene expression in response to signal binding.

23 AHL signals share a conserved lactone core, but vary in the acyl moiety which can be a fatty  
24 acid ranging from 4 to 20 carbons long, with potential oxidation on the C3 carbon and varying degrees  
25 of unsaturation, or can have an aromatic or branched structure<sup>8</sup>. This variability in the acyl portion of the  
26 signal confers selectivity to the system. Typically, a LuxI-type synthase produces a primary AHL to  
27 which its paired LuxR-type receptor selectively responds<sup>9</sup>. Selectivity is critical to cell signaling in order  
28 to avoid undesired cross-talk or spurious outputs<sup>10</sup>. In the case of QS, selectivity ensures bacteria  
29 cooperate only with kin cells.

30 Despite its importance, we know little about how QS systems achieve selectivity or how they  
31 evolve and diversify to use new signals. Although the conserved amino acids essential for synthase and  
32 receptor activity are well described<sup>11,12</sup>, residues that dictate selectivity are often different from those  
33 that are required for activity<sup>13</sup>. Due to the low amino acid sequence identity between LuxI/R  
34 homologues, it has been difficult to determine how QS systems discriminate between various AHL  
35 signals<sup>14</sup>.

36 We hypothesized that we could use covariation patterns to identify QS selectivity residues. Such  
37 methods have been used to identify amino acid residues that interact with each other within proteins and  
38 between proteins that physically bind each other<sup>15-17</sup>. Here, we endeavored to expand these methods to  
39 assess the interaction between AHL synthases and receptors. While AHL synthases and receptors do not  
40 physically interact, they interact indirectly via binding to a shared cognate signal and are believed to  
41 coevolve to maintain this shared signal recognition<sup>9</sup>. Phylogenetic analyses also support coevolution of  
42 synthases and receptors<sup>18,19</sup>. We therefore hypothesized that we could identify amino acid residues that  
43 covary between QS synthases and receptors, and further, that the covarying residues would be those  
44 responsible for signal selectivity.

45 We used a statistical method, GREMLIN<sup>20</sup>, to measure covariation within the sequences of AHL  
46 synthase-receptor pairs and mapped the covarying residues onto the LasI/R QS system of *Pseudomonas*  
47 *aeruginosa* PAO1. By mutating the top-scoring residues identified by GREMLIN, we demonstrate that  
48 they are indeed important for signal selectivity and, further, that these residues can be used to rationally  
49 engineer LasI/R to produce and respond to a non-native signal. We thus demonstrate a new application  
50 for powerful covariation methods and at the same time identify determinants of QS selectivity.

## 51 **Results**

52 **Covariation patterns in QS systems.** To begin our analysis, we gathered select protein sequences for  
53 known synthase-receptor pairs (Supplementary Table 1) and used these sequences to search the  
54 European Nucleotide Archive (ENA) database<sup>21</sup> from the European Bioinformatics Institute and the  
55 Integrated Microbial Genomes and Microbiomes (IMG/M) database<sup>22</sup> from the Joint Genome Institute  
56 (JGI) for additional synthase-receptor pairs. The genes for synthase-receptor pairs are frequently co-  
57 located on the genome, and organisms can harbor more than one complete QS system<sup>14</sup>. To increase the  
58 likelihood of identifying true pairs, we required that the two genes be separated by no more than two

59 coding sequences. A total of 6,360 non-identical pairs were identified. We further discarded pairs that  
60 were more than 90% identical to another pair, resulting in 3,489 representative AHL synthase-receptor  
61 pairs.

62 We aligned these sequences to the LasI/R QS system from *P. aeruginosa* PAO1. Not only is *P.*  
63 *aeruginosa* a clinically important pathogen, the Las system is well-studied and crystal structures have  
64 been solved for both LasI<sup>23</sup> and LasR<sup>24</sup>, making this a particularly useful model system for our studies.  
65 We connected the sequences of synthase and receptor from each pair and used GREMLIN to analyze  
66 covariation patterns in these sequences (Supplementary Fig. 1). We applied Average Product Correction  
67 (APC) to the GREMLIN covariance coefficients, a common technique shown to improve the accuracy  
68 of coevolution analyses<sup>25</sup>. We performed the same analysis by aligning the synthase-receptor pairs to the  
69 LuxI/R system from *Vibrio fischeri* MJ11. The top-ranking coevolving residue pairs overlap  
70 significantly between the LasI/R and LuxI/R systems (62.5% in common among the top 0.05% residue  
71 pairs) (Supplementary Fig. 1). We integrated the analyses for the LasI/R and LuxI/R systems by using  
72 the higher score for each residue pair and the top 10 residue pairs are shown in Fig. 2a. As a control, we  
73 randomly paired the synthases and receptors from different species and reanalyzed them using  
74 GREMLIN. While top-scoring covarying residues had a minimal GREMLIN score (with APC) of 0.09,  
75 the highest score from the randomized control was 0.08 (Fig. 2b). This control provides a guideline for  
76 our analysis; residues with a GREMLIN score (with APC) above or near the maximal score for the  
77 randomized control are likely to be meaningful.

78 **Top-scoring residues cluster near ligand-binding pockets.** For both LasI and LasR, the top-scoring  
79 covarying residues cluster around the ligand-binding pocket. For LasR, the top-scoring residues map  
80 exclusively to the ligand-binding domain with an average distance of 5.0 Å from the co-crystallized  
81 native ligand *N*-3-oxo-dodecanoyl-L-homoserine lactone (3OC12-HSL) (Fig. 2c). In contrast, the

82 residues identified in the randomized control are scattered throughout LasR, including three residues in  
83 the DNA-binding domain, and are an average distance of 17.8 Å from 3OC12-HSL (Fig. 2d).

84 In LasI, the top-scoring covarying residues cluster around the hydrophobic pocket thought to bind  
85 the fatty acyl substrate (Fig. 2e) and are an average distance of 3.7 Å from an acyl substrate modeled  
86 into the LasI structure<sup>23</sup>. As with LasR, the residues identified in the randomized control are scattered  
87 throughout LasI, with many of the residues exposed to solvent (Fig. 2f). The randomized control  
88 residues in LasI are over three times further from the fatty acyl substrate, mean distance = 11.7Å,  
89 compared to the covarying residues.

90 Due to their location near the ligand-binding pockets, several of the covarying residues have been  
91 previously studied in various LasI/R homologues. Encouragingly, many of these residues have been  
92 reported to be important for protein activity and, in some cases, for selectivity. We have summarized  
93 several of these studies in Supplementary Tables 2 and 3.

94 **LasR mutations alter selectivity.** To determine whether residues identified by GREMLIN are involved  
95 in LasR selectivity, we mutated a selection of the top-scoring amino acids, G38, R61, A127, S129, and  
96 L130, to the most common natural variants at each position (Supplementary Table 4). By expressing  
97 LasR in *Escherichia coli* and measuring its activity against a previously reported panel of 19 AHL  
98 signals<sup>26</sup>, we were able to quickly prioritize mutants for further study. The majority of our LasR mutants  
99 retained the ability to respond to AHLs and all mutants had an altered selectivity profile when compared  
100 to wild-type (Supplementary Fig. 2).

101 We, and others, have previously demonstrated that compared to native activity, QS receptor  
102 sensitivity and selectivity can be altered when in *E. coli*<sup>26,27</sup>. We therefore engineered several mutations  
103 into *lasR* on the *P. aeruginosa* PAO-SC4 chromosome to confirm our findings. *P. aeruginosa* PAO-SC4  
104 is an AHL synthase-null mutant which we use here to measure LasR activity in response to exogenously

105 provided AHL signals. The *lasR* mutations largely had the same effect on activity and selectivity in *P.*  
106 *aeruginosa* as they did when *lasR* was expressed *E. coli* (Supplementary Fig. 3). Of note, LasR<sup>A127L</sup> had  
107 an increased sensitivity to numerous signals (Fig. 3a-d), potentially through increased hydrophobic  
108 interactions with the fatty acyl chain of the AHLs. Consistent with its role in a water-mediated hydrogen  
109 bond with the C3 oxygen of 3OC12-HSL, and with previous studies<sup>28,29</sup>, LasR R61 mutants were less  
110 responsive to oxo-substituted AHLs, but maintained wild-type or better levels of activation by  
111 unsubstituted AHLs (Fig. 3a-d and Supplementary Fig. 3).

112 The mutations also affected the sensitivity of LasR to 3OC12-HSL (Supplementary Fig. 3).  
113 Interestingly, two of our mutants were more sensitive to 3OC12-HSL than wild-type LasR. LasR<sup>A127L</sup>  
114 was roughly 3-fold more sensitive and LasR<sup>L130F</sup> was 2-fold more sensitive (Fig. 3e). This increased  
115 sensitivity came at the cost of decreased selectivity for both of these mutations. In fact, many of our  
116 single amino acid mutants displayed reduced selectivity compared to wild-type LasR (Supplementary  
117 Fig. 2 and Supplementary Fig. 3).

118 **LasI mutations alter activity and selectivity.** Similar to LasR, we focused our LasI mutations on the  
119 top-scoring positions: L102, T142, T145, and L157 (Supplementary Table 5). We expressed wild-type  
120 or mutated *lasI* on a low copy number plasmid in the AHL synthase-null *P. aeruginosa* PAO-SC4 and  
121 extracted AHLs produced by these bacteria from culture fluid. While bioassays are commonly used for  
122 the detection of AHLs<sup>30</sup>, they suffer from multiple drawbacks. In particular, bioassays are not equally  
123 sensitive to all AHLs and typically cannot be used to determine which AHLs are produced and in what  
124 ratio. To screen our LasI mutants for altered activity and selectivity, we developed a thin layer  
125 chromatography (TLC) method based on our existing high performance liquid chromatography (HPLC)  
126 radiotracer assay<sup>31</sup>. In this method, the C1 position in the homoserine lactone ring is labeled with <sup>14</sup>C.  
127 The label is incorporated into AHLs at a ratio of one <sup>14</sup>C per AHL molecule. This results in unbiased

128 detection of all AHLs produced. While the established method uses HPLC to separate and detect AHLs  
129 one sample at a time, we can run nine samples per TLC, resulting in a more high-throughput assay.

130 Using our TLC method, we confirmed that *lasI* directs the synthesis of the same primary product  
131 whether it is expressed on a plasmid or from the chromosome (Supplementary Fig. 4). HPLC analysis of  
132 matched extracts confirmed that the major LasI product observed by TLC is 3OC12-HSL. As expected,  
133 an empty vector control did not produce detectable AHLs, nor did we detect radioactivity in a media-  
134 only control. We then screened the activity each *lasI* mutant by TLC (Supplementary Fig. 4). Several  
135 mutants produced little or no detectable AHLs, while some appeared to produce more 3OC12-HSL than  
136 wild-type LasI. We analyzed select extracts by both TLC and HPLC and found that the results were  
137 consistent between the two methods, further validating the TLC method.

138 Based on our TLC results we selected one mutant, LasI<sup>L157W</sup>, for further study by HPLC. We  
139 found that LasI<sup>L157W</sup> produces equal amounts of two <sup>14</sup>C-AHLs that elute in the fractions of *N*-3-oxo-  
140 decanoyl-L-homoserine lactone (3OC10-HSL) and *N*-3-oxo-octanoyl-L-homoserine lactone (3OC8-  
141 HSL) along with a lesser amount of 3OC12-HSL (Fig. 4). These findings demonstrate that the covarying  
142 residues influence LasI activity and selectivity, and that a single mutation is sufficient to significantly  
143 alter LasI selectivity.

144 **Multiple mutations can “rewire” LasI/R selectivity.** In general, multiple mutations are required to  
145 generate a protein with orthogonal selectivity<sup>15,17,28</sup>. In non-QS proteins, altered selectivity has been  
146 engineered by swapping the covarying residues in one homolog to the identities in another<sup>15,17</sup>. Here, we  
147 seek to “rewire” LasI/R to use an orthogonal signal. We targeted the MupI/R system from *Pseudomonas*  
148 *fluorescens* NCIMB 10586, which uses the signal 3OC10-HSL<sup>32</sup>. MupI and MupR share 52% and 39%  
149 identity with LasI and LasR, respectively.



150 LasR and MupR differ at eight covariation sites in the ligand-binding domain with a GREMLIN  
151 score (with APC) > 0.08 (Supplementary Fig. 5). LasR modified to contain all eight mutations was  
152 inactive. However, there were several intermediate mutants that displayed an increased response to  
153 3OC10-HSL. We identified three mutations that are sufficient for this increased sensitivity: L125F,  
154 A127M, and L130F (Fig. 5a). LasR<sup>L125F, A127M, L130F</sup> is over 20-fold more sensitive to 3OC10-HSL than  
155 wild-type LasR. The L125F mutation appears to be the primary driver of this altered selectivity (Fig.  
156 5b,c and Supplementary Fig. 5). All “MupR-like” LasR mutants responded to 3OC12-HSL with similar  
157 sensitivity to wild-type LasR (Supplementary Fig. 5).

158 LasI differs from MupI at five high-scoring covariation residues: LasI M125, T145, M152, V159,  
159 and N181 (Supplementary Fig. 6), the first 3 of which line the LasI acyl-binding pocket (Fig. 5d).  
160 Swapping these three residues for their MupI identities resulted in a synthase that has substantially  
161 altered selectivity. LasI<sup>M125I, T145S, M152L</sup> produces ~2-fold more 3OC10-HSL than 3OC12-HSL (Fig. 5e).  
162 The M125I mutation alone was sufficient to relax LasI’s selectivity, resulting in a synthase that produces  
163 roughly equal amounts of 3OC10-HSL and 3OC12-HSL. As a comparison, we measured the activity of  
164 *mupI* expressed in *P. aeruginosa*, and found it produces 9:1 3OC10-HSL:3OC12-HSL (Fig. 5e and  
165 Supplementary Fig. 6). All single and double “MupI-like” LasI mutants retained AHL synthase activity,  
166 but only those mutants that contain the M125I mutation displayed increased 3OC10-HSL production  
167 relative to 3OC12-HSL (Supplementary Fig. 6).

## 168 Discussion

169 Despite decades of study, it has been challenging to determine how AHL QS systems distinguish  
170 between signals. We hypothesized that we could identify covariation patterns in AHL QS systems and  
171 that these patterns would illuminate residues important for signal selectivity. By analyzing the sequences  
172 of 6,360 unique QS systems, we identified amino acids that strongly covary between AHL synthases and

173 receptors. The top-scoring residues in our analysis cluster near the ligand-binding pockets for both  
174 proteins and are more than three times closer to the signal molecule compared to top-scoring residues in  
175 a randomized control. We focused our study on *P. aeruginosa* LasI/R. Through targeted mutations in the  
176 top-scoring covarying residues we demonstrate that these amino acids are indeed determinants of signal  
177 selectivity. We have thus validated a new application of covariation analysis for proteins that interact  
178 indirectly and not through direct binding to one-another. Additionally, these strong covariation results  
179 further support the view that AHL synthases and receptors coevolve.

180 For both the synthase, LasI, and the receptor, LasR, a single amino acid substitution is sufficient  
181 to significantly alter selectivity. Interestingly, our mutations also revealed that LasR is not optimized to  
182 be as sensitive as possible to its native 3OC12-HSL signal. The increase in sensitivity of specific  
183 mutants came at the cost of decreased selectivity, which suggests that QS systems may evolve to balance  
184 these two properties. Furthermore, increased sensitivity to the native signal may lead to premature  
185 activation of the QS regulon, which would likely decrease fitness<sup>33</sup>. The mutants generated in our study  
186 provide us with the tools to directly address these questions and assess the impact of sensitivity and  
187 selectivity on QS function.

188 We also demonstrated that we can use covarying residues to rationally engineer a QS system to  
189 produce and respond to a signal of our choosing. By mutating the covarying residues in LasI/R, we  
190 improved the sensitivity of LasR to 3OC10-HSL over 20-fold and increased the production of 3OC10-  
191 HSL by LasI roughly 15-fold. For both the synthase and receptor, a single amino acid substitution was  
192 the primary driver of the altered selectivity. This was surprising given the low sequence identity between  
193 LasI/R and MupI/R. These findings suggest new QS systems might evolve with relative ease. Further,  
194 the ability to engineer QS selectivity could be beneficial to synthetic biology where AHL signaling is a  
195 powerful tool to build biological circuits<sup>34</sup>.

196        Though we were able to substantially increase the 3OC10-HSL activity of LasI/R, our mutants  
197 retained their native 3OC12-HSL activity. We have thus generated a promiscuous system with  
198 broadened selectivity. Similarly, a directed evolution study of the AHL receptor LuxR found that it  
199 evolves through promiscuous intermediates<sup>13</sup>. This has also been observed in other systems, such as  
200 toxin-antitoxin systems<sup>17</sup>. Proteins tend to evolve through broadly active intermediates before gaining  
201 new specificity. In this way, the system maintains functionality *en route* to altered selectivity. Quorum  
202 sensing systems appear to follow these same trends.

203        One limitation we faced is a lack of close LasI/R homologs with known signals. It has been  
204 demonstrated that “supporting” residues, i.e. residues within a protein that covary with the selectivity  
205 residues, may indirectly impact selectivity by influencing the orientation of selectivity residues<sup>17</sup>. Thus,  
206 given the large differences in sequence identity between the Las and Mup systems, there are likely other  
207 residues that must be mutated to fully swap selectivity. The identification of a more closely related  
208 system to LasI/R may provide a better starting point for engineering altered selectivity. Alternatively,  
209 our mutants could be further evolved through saturating mutagenesis and/or *in vitro* evolution.

210        Collectively, our results provide insight into AHL QS selectivity and will help us predict signal  
211 selectivity in newly identified QS systems, in metagenomes, and in naturally occurring QS variants such  
212 as those found in clinical isolates. More broadly, we have gained insight into how AHL QS systems  
213 evolve and diversify.

## 214 **Methods**

215 **Identification of quorum sensing systems.** Starting from 24 pairs of manually curated QS synthases  
216 and receptors (Supplementary Table 1), we searched for homologs in complete bacterial genomes using  
217 BLAST (e-value <0.01)<sup>35</sup>. We filtered the BLAST hits by sequence identity (>30%) to the query and the  
218 alignment coverage (query coverage >0.75 and hit coverage >0.75), and the filtered hits were aligned by

219 Clustal Omega<sup>36</sup>. We selected the LasI/R system from *Pseudomonas aeruginosa* PAO1 as the target and  
220 mapped the Multiple Sequence Alignments (MSA) to the target system. We built sequence profiles from  
221 the MSA with HMMER<sup>37</sup> and hmmbuild for the QS synthases and receptors, respectively. The sequence  
222 profiles were then used to search against the European Nucleotide Archive database<sup>21</sup> and the Integrated  
223 Microbial Genomes and Microbiomes database<sup>22</sup> from Joint Genome Institute using HMMER  
224 hmmsearch. A total of 149,837 and 5,046,620 homologs were found in these databases for the QS  
225 synthase and receptor, respectively. Because the synthases and receptors of the known QS systems  
226 frequently locate near each other in the genome, we kept synthase-receptor gene pairs that are separated  
227 by no more than two other open reading frames (ORFs) in the genome or contig. A total of 14,980  
228 synthase-receptor gene pairs were identified and they represent 6,360 non-identical QS systems. In  
229 another attempt, we carried out the same procedure using the LuxI/R system from *Vibrio fischeri* MJ11  
230 as the target system. A similar number of QS systems were identified.

231 **Identification of covarying residues.** We connected the synthase and receptor protein sequences for  
232 each QS system we found in the databases and derived the alignments between these QS systems to the  
233 target QS system (LasI/R) from the hmmsearch result. We filtered the MSA for synthase-receptor pairs  
234 by sequence identity (maximal identify for remaining sequences  $\leq 90\%$ ) and gap ratio in each sequence  
235 (maximal gap ratio  $\leq 25\%$ ). We applied GREMLIN to analyze the covariation in the MSA<sup>20</sup>, and the  
236 GREMLIN coefficients were normalized using Average Product Correction (APC)<sup>25</sup> as we described  
237 previously<sup>16</sup>. The GREMLIN coefficients after APC were used as measures for covariation signals  
238 between synthase and receptor amino acid residues. As a control, we connected each synthase sequence  
239 with a randomly selected receptor sequence and performed the covariation analysis in the same way.

240 We mapped the top-scoring covarying residues in the LasI/R system onto the crystal structures  
241 for each protein. Reported distances between residues and ligands are the shortest distance between any

242 non-hydrogen atoms. For LasR, distances were calculated using PDB 6V7X. For LasI, distances were  
243 calculated using a LasI structure with 3-oxo-C12-acyl-phosphopantetheine modeled into the acyl-  
244 binding pocket<sup>23</sup>. Reported distances for LasI are between residues and the acyl portion of the modeled  
245 substrate.

246 **Bacterial strains, plasmids, and culture conditions.** Bacterial strains and plasmids are listed in  
247 Supplementary Table 6. Unless otherwise specified, *Pseudomonas aeruginosa* and *Escherichia coli*  
248 were grown in lysogeny broth (LB) (10 g tryptone, 5 g yeast extract, 5 g NaCl per liter) buffered with 50  
249 mM 3-(*N*-morpholino) propanesulfonic acid (MOPS) (pH 7) (LB/MOPS) or on LB agar (LB plus 1.5%  
250 Bacto agar)<sup>26</sup>. Liquid cultures were grown at 37°C with shaking. For radiotracer thin layer  
251 chromatography (TLC) experiments, *P. aeruginosa* was grown in Jensen's medium with 0.3%  
252 glycerol<sup>31</sup>.

253 For plasmid selection and maintenance, antibiotics were used at the following concentrations: *P.*  
254 *aeruginosa*, 30 µg per mL gentamicin (Gm) and 150 µg per mL carbenicillin (Cb); *E. coli* 10 µg per mL  
255 Gm and 100 µg per mL ampicillin (Ap). BD Difco *Pseudomonas* Isolation Agar (PIA) was prepared  
256 according to manufacturer directions and supplemented with 100 µg per mL Gm as needed. Where  
257 needed for gene expression L-arabinose (0.4% w/v) was added.

258 All chemicals and reagents were obtained from commercial sources. AHLs were dissolved either  
259 in dimethyl sulfoxide (DMSO) or in ethyl acetate (EtAc) acidified with glacial acetic acid (0.01% v/v).  
260 AHLs in DMSO were used at ≤1% of the final culture volume and AHLs dissolved in EtAc were dried  
261 on the bottom of the culture vessel prior to addition of the bacterial culture. DMSO or acidified EtAc  
262 was used as a vehicle control where appropriate.

263 **Plasmid and strain construction.** pJN-lasI and pJN-RBSmupI were constructed using *E. coli*-mediated  
264 DNA assembly<sup>38</sup>. Briefly, for pJN-lasI, *lasI* was amplified from *P. aeruginosa* PAO1 genomic DNA

265 (gDNA) using primers lasI-pJN-F and lasI-pJN-R (Supplementary Table 6). pJN105 was amplified  
266 using the reverse complement of these primers. The resulting PCR products were treated with the  
267 restriction enzyme DpnI to remove the parent template. Both PCR products were then used to transform  
268 *E. coli* (NEB 5alpha). The resulting constructs were confirmed by Sanger sequencing. For pJN-  
269 RBSmupI, we began by amplifying *mupI* from *Pseudomonas fluorescens* Migula (ATCC 49323) gDNA  
270 using primers mupI-F and mupI-R. We then used primers mupI-pJN-F and mupI-pJN-R to amplify the  
271 *mupI* PCR product and used the reverse complement of these two primers to amplify pJN-RBSlasI. The  
272 resulting PCR products were treated the same as for pJN-lasI. We constructed pJN-RBSlasI using  
273 restriction digestion. The *lasI* gene, including its upstream ribosomal binding site (RBS), was amplified  
274 from *P. aeruginosa* PAO1 gDNA using primers RBS-lasI-F and lasI-pJN-R. pJN-lasI and the RBS-*lasI*  
275 PCR product were digested using NheI and SacI, gel or column purified respectively, ligated by T4  
276 DNA ligase, and transformed into NEB 5alpha. The resulting constructs were confirmed by Sanger  
277 sequencing. Plasmids were introduced into *E. coli* by using heat shock and were introduced into *P.*  
278 *aeruginosa* by electroporation.

279 Point-mutations were introduced to *lasI* and *lasR* on pJN-lasI and JNL or pEXG2-lasR,  
280 respectively, using site directed mutagenesis by PCR. Primers were designed to amplify each plasmid  
281 while introducing the desired mutation(s). The resulting PCR products were treated with DpnI and were  
282 then used to transform NEB 5alpha. Plasmids from the resulting colonies were screened for the desired  
283 mutations by Sanger sequencing. To mutate *lasR* on the *P. aeruginosa* PAO-SC4 chromosome, *E. coli*  
284 S17-1 was used to deliver pEXG2-lasR containing various *lasR* mutations to PAO-SC4 via conjugation  
285 and potential mutants were isolated as previously described<sup>39</sup>. All mutations were confirmed by PCR  
286 amplification of *lasR* from the genome followed by Sanger sequencing.

287 **LasR activity measurements.** LasR activity was measured in *E. coli* containing pJNL and pPROBE-  
288 P<sub>rsaL</sub> or in *P. aeruginosa* PAO-SC4 containing pPROBE-P<sub>rsaL</sub> using previously reported methods<sup>26</sup>.  
289 Briefly, overnight-grown cultures were diluted 1:100 and grown back to log-phase. For *E. coli*, cultures  
290 were grown to an optical density at 600 nm (OD) of 0.3, treated with L-arabinose (0.4%), and incubated  
291 with AHLs for 4 h. For *P. aeruginosa*, cultures were grown to an OD between 0.05 and 0.3, were diluted  
292 to an OD of 0.01 and then incubated with AHLs for 16 to 18 h. LasR activity was measured as GFP  
293 fluorescence (excitation 490 nm, emission 520 nm, gain 50) using a Synergy H1 microplate reader  
294 (Biotek Instruments). Activity measurements were normalized by dividing by OD and subtracting  
295 background values (fluorescence per OD for cultures incubated with vehicle control). Concentrations of  
296 half maximal activation, EC<sub>50</sub>, were calculated using GraphPad Prism.

297 **TLC screening for AHLs.** Cultures of *P. aeruginosa* PAO1Δ*rhII* or of *P. aeruginosa* PAO-SC4 with  
298 pJN-empty or with wild-type or mutated pJN-*lasI* were grown overnight in Jensen's medium with 0.3%  
299 glycerol. Overnight cultures were used to inoculate fresh medium (1% v/v). When the OD reached 0.5,  
300 *lasI* expression was induced with arabinose (0.4%) and 1.1 mL cultures were incubated with 1.1 μCi/mL  
301 L-[1-<sup>14</sup>C]-methionine (<sup>14</sup>C-methionine) for 90 min<sup>31</sup>. Cells were pelleted by centrifugation and 1 mL of  
302 supernatant fluid was extracted twice with 2 mL acidified EtAc. The extracts were dried under N<sub>2</sub> and  
303 resuspended in 15 μL acidified EtAc. Five μL of each extract was spotted on an aluminum backed C18-  
304 W-silica TLC plate (Sorbtech). AHLs were separated using 70% methanol in water, then the TLC plate  
305 was dried and exposed to a phosphor screen for at least 16 h. Phosphor screens were imaged with a  
306 Sapphire Biomolecular Imager (Azure Biosystems). To confirm TLC findings, select extracts were  
307 dried, suspended in methanol and analyzed by C18-reversed-phase high performance liquid  
308 chromatography (HPLC) using a previously reported method<sup>31</sup>.

309 **HPLC radiotracer assays for LasI activity.** For better detection of AHLs, we slightly modified the  
310 radiolabeling protocol detailed above, modeling it after a previously published method<sup>40</sup>. Cultures of *P.*  
311 *aeruginosa* PAO-SC4 with wild-type or mutated pJN-RBS<sub>1</sub>lasI were grown overnight in LB/MOPS.  
312 Overnight cultures were used to inoculate 5 mL LB/MOPS (1% v/v). After 2 h, *lasI* expression was  
313 induced with arabinose (0.4%) and cultures were grown to OD 0.7. Cells were centrifuged at 5,000 rpm  
314 for 10 min, and pellets were suspended in 1.1 mL phosphate buffered saline (PBS) with 10 mM glucose.  
315 After shaking incubation at 37°C for 10 min, 1.1 μCi <sup>14</sup>C-methionine was added to the cell suspension.  
316 Cell suspensions were incubated with radiolabel for 2 h, after which cells were pelleted by  
317 centrifugation and 1 mL supernatant fluid was extracted twice with 2 mL acidified EtAc. Radiolabeled  
318 AHLs were dried under N<sub>2</sub> and suspended in methanol. One-third of each extract was analyzed by  
319 reversed-phase HPLC using a gradient of 10 to 100% methanol-in-water<sup>31</sup>.



320 **References**

321

- 322 1. Whiteley, M., Diggle, S.P. & Greenberg, E.P. Progress in and promise of bacterial quorum sensing  
323 research. *Nature* **551**, 313-320 (2017).
- 324 2. Waters, C.M. & Bassler, B.L. Quorum sensing: Cell-to-cell communication in bacteria. *Annu. Rev.*  
325 *Cell Dev. Biol.* **21**, 319-346 (2005).
- 326 3. Case, R.J., Labbate, M. & Kjelleberg, S. AHL-driven quorum-sensing circuits: Their frequency and  
327 function among the Proteobacteria. *ISME J.* **2**, 345-349 (2008).
- 328 4. Mellbye, B.L. *et al.* Acyl-homoserine lactone production in nitrifying bacteria of the genera  
329 *Nitrospira*, *Nitrobacter*, and *Nitrospira* identified via a survey of putative quorum-sensing  
330 genes. *Appl. Environ. Microbiol.* **83**, e01540-01517 (2017).
- 331 5. Schaefer, A.L. *et al.* A new class of homoserine lactone quorum-sensing signals. *Nature* **454**, 595-  
332 599 (2008).
- 333 6. Kaplan, H.B. & Greenberg, E.P. Diffusion of autoinducer is involved in regulation of the *Vibrio*  
334 *fischeri* luminescence system. *J. Bacteriol.* **163**, 1210 (1985).
- 335 7. Pearson, J.P., Van Delden, C. & Iglewski, B.H. Active efflux and diffusion are involved in transport  
336 of *Pseudomonas aeruginosa* cell-to-cell signals. *J. Bacteriol.* **181**, 1203 (1999).
- 337 8. Rajput, A., Kaur, K. & Kumar, M. SigMol: Repertoire of quorum sensing signaling molecules in  
338 prokaryotes. *Nucleic Acids Res.* **44**, D634-639 (2016).
- 339 9. Aframian, N. & Eldar, A. A bacterial tower of babel: Quorum-sensing signaling diversity and its  
340 evolution. *Annu. Rev. Microbiol.* **74**, 587-606 (2020).
- 341 10. Laub, M.T. Keeping signals straight: How cells process information and make decisions. *PLoS Biol.*  
342 **14**, e1002519 (2016).
- 343 11. Parsek, M.R., Schaefer, A.L. & Greenberg, E.P. Analysis of random and site-directed mutations in  
344 *rhlI*, a *Pseudomonas aeruginosa* gene encoding an acylhomoserine lactone synthase. *Mol.*  
345 *Microbiol.* **26**, 301-310 (1997).
- 346 12. Zhang, R.-G. *et al.* Structure of a bacterial quorum-sensing transcription factor complexed with  
347 pheromone and DNA. *Nature* **417**, 971-974 (2002).
- 348 13. Collins, C.H., Arnold, F.H. & Leadbetter, J.R. Directed evolution of *Vibrio fischeri* LuxR for  
349 increased sensitivity to a broad spectrum of acyl-homoserine lactones. *Mol. Microbiol.* **55**, 712-  
350 723 (2005).
- 351 14. Fuqua, C., Winans, S.C. & Greenberg, E.P. Census and consensus in bacterial ecosystems: The  
352 LuxR-LuxI family of quorum-sensing transcriptional regulators. *Annu. Rev. Microbiol.* **50**, 727-  
353 751 (1996).

- 354 15. Skerker, J.M. *et al.* Rewiring the specificity of two-component signal transduction systems. *Cell*  
355 **133**, 1043-1054 (2008).
- 356 16. Ovchinnikov, S., Kamisetty, H. & Baker, D. Robust and accurate prediction of residue–residue  
357 interactions across protein interfaces using evolutionary information. *eLife* **3**, e02030 (2014).
- 358 17. Aakre, C.D. *et al.* Evolving new protein-protein interaction specificity through promiscuous  
359 intermediates. *Cell* **163**, 594-606 (2015).
- 360 18. Gray, K.M. & Garey, J.R. The evolution of bacterial LuxI and LuxR quorum sensing regulators.  
361 *Microbiology* **147**, 2379-2387 (2001).
- 362 19. Lerat, E. & Moran, N.A. The evolutionary history of quorum-sensing systems in bacteria. *Mol. Biol.*  
363 *Evol.* **21**, 903-913 (2004).
- 364 20. Kamisetty, H., Ovchinnikov, S. & Baker, D. Assessing the utility of coevolution-based residue–  
365 residue contact predictions in a sequence- and structure-rich era. *PNAS* **110**, 15674 (2013).
- 366 21. Amid, C. *et al.* The European Nucleotide Archive in 2019. *Nucleic Acids Res.* **48**, D70-D76 (2019).
- 367 22. Chen, I.-M.A. *et al.* The IMG/M data management and analysis system v.6.0: New tools and  
368 advanced capabilities. *Nucleic Acids Res.* **49**, D751-D763 (2020).
- 369 23. Gould, T.A., Schweizer, H.P. & Churchill, M.E.A. Structure of the *Pseudomonas aeruginosa* acyl-  
370 homoserinelactone synthase LasI. *Mol. Microbiol.* **53**, 1135-1146 (2004).
- 371 24. Zou, Y. & Nair, S.K. Molecular basis for the recognition of structurally distinct autoinducer mimics  
372 by the *Pseudomonas aeruginosa* LasR quorum-sensing signaling receptor. *Chem. Biol.* **16**, 961-  
373 970 (2009).
- 374 25. Buslje, C.M. *et al.* Correction for phylogeny, small number of observations and data redundancy  
375 improves the identification of coevolving amino acid pairs using mutual information.  
376 *Bioinformatics* **25**, 1125-1131 (2009).
- 377 26. Wellington, S. & Greenberg, E.P. Quorum sensing signal selectivity and the potential for  
378 interspecies cross talk. *mBio* **10**, e00146-00119 (2019).
- 379 27. Moore, J.D. *et al.* A comparative analysis of synthetic quorum sensing modulators in *Pseudomonas*  
380 *aeruginosa*: New insights into mechanism, active efflux susceptibility, phenotypic response, and  
381 next-generation ligand design. *J. Am. Chem. Soc.* **137**, 14626-14639 (2015).
- 382 28. Collins, C.H., Leadbetter, J.R. & Arnold, F.H. Dual selection enhances the signaling specificity of a  
383 variant of the quorum-sensing transcriptional activator LuxR. *Nat. Biotechnol.* **24**, 708-712  
384 (2006).
- 385 29. Gerdt, J.P. *et al.* Unraveling the contributions of hydrogen-bonding interactions to the activity of  
386 native and non-native ligands in the quorum-sensing receptor LasR. *Org. Biomol. Chem.* **13**,  
387 1453-1462 (2015).

- 388 30. Chu, W. *et al.* Bioassays of quorum sensing compounds using *Agrobacterium tumefaciens* and  
389 *Chromobacterium violaceum* in *Quorum Sensing: Methods and Protocols* Vol. 692 Ch. 1  
390 (Humana Press, Totowa, NJ, 2011).
- 391 31. Schaefer, A.L., Harwood, C.S. & Greenberg, E.P. “Hot Stuff”: The many uses of a radiolabel assay  
392 in detecting acyl-homoserine lactone quorum-sensing signals in *Quorum Sensing: Methods and*  
393 *Protocols* Vol. 1673 Ch. 3 (Springer New York, New York, NY, 2018).
- 394 32. Hothersall, J. *et al.* Manipulation of quorum sensing regulation in *Pseudomonas fluorescens*  
395 NCIMB 10586 to increase mupirocin production. *Appl. Microbiol. Biotechnol.* **90**, 1017-1026  
396 (2011).
- 397 33. Darch, S.E. *et al.* Density-dependent fitness benefits in quorum-sensing bacterial populations. *PNAS*  
398 **109**, 8259-8263 (2012).
- 399 34. Davis, R.M., Muller, R.Y. & Haynes, K.A. Can the natural diversity of quorum-sensing advance  
400 synthetic biology? *Front. Bioeng. Biotechnol.* **3**, e1-e30 (2015).
- 401 35. Altschul, S.F. *et al.* Basic local alignment search tool. *J. Mol. Biol.* **215**, 403-410 (1990).
- 402 36. Sievers, F. & Higgins, D.G. The clustal omega multiple alignment package. *Methods Mol. Biol.*  
403 **2231**, 3-16 (2021).
- 404 37. Eddy, S.R. A new generation of homology search tools based on probabilistic inference. *Genome*  
405 *Inform.* **23**, 205-211 (2009).
- 406 38. Kostylev, M. *et al.* Cloning should be simple: *Escherichia coli* DH5 $\alpha$ -mediated assembly of  
407 multiple DNA fragments with short end homologies. *PLoS One* **10**, e0137466 (2015).
- 408 39. Kostylev, M. *et al.* Evolution of the *Pseudomonas aeruginosa* quorum-sensing hierarchy. *PNAS*  
409 **116**, 7027 (2019).
- 410 40. Leadbetter, J.R. & Greenberg, E.P. Metabolism of acyl-homoserine lactone quorum-sensing signals  
411 by *Variovorax paradoxus*. *J. Bacteriol.* **182**, 6921-6926 (2000).

412

413 **Acknowledgements**

414 We thank Mair Churchill for sharing her lab's LasI structure modeled with an acyl substrate. This work  
415 was supported by grants NIH R35GM136218 to EPG, Yeast Program Grant 5 P41 GM103533-24,  
416 Washington Research Foundation fellowship to QC, and Helen Hay Whitney Foundation fellowship to  
417 SWM.

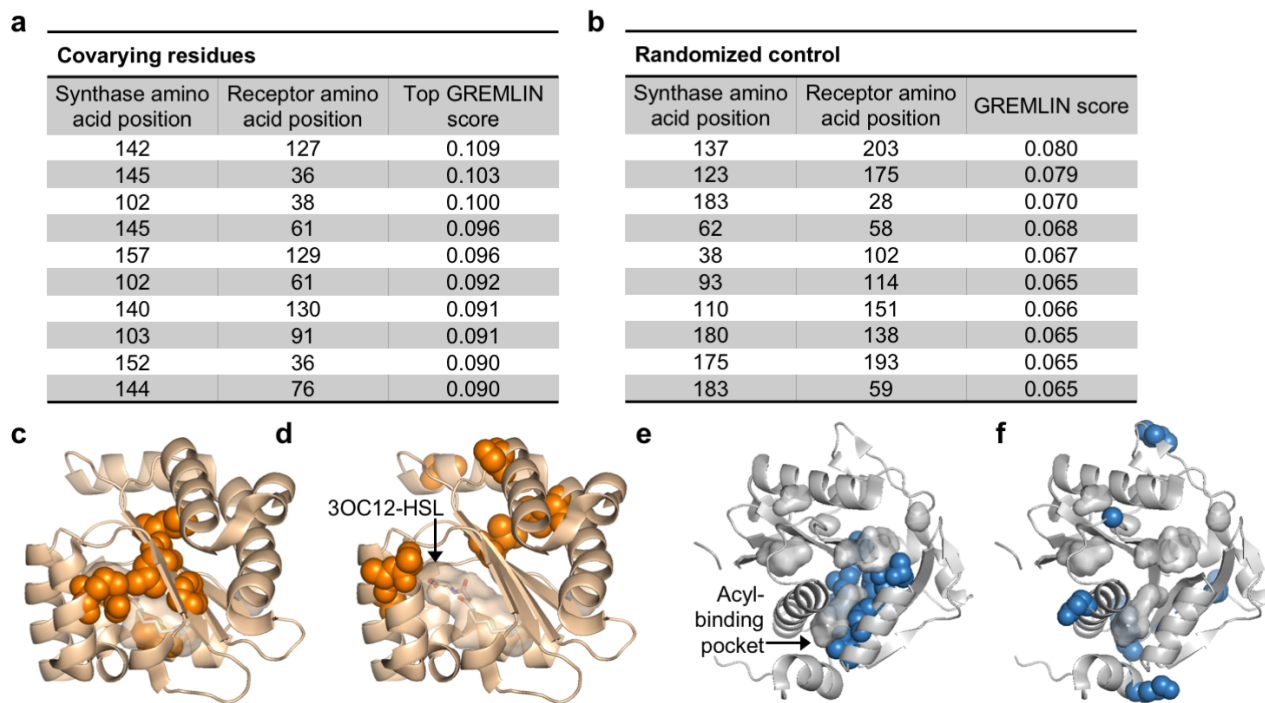
418 **Author contributions**

419 SWM, QC, DB, and EPG conceived of and designed the investigation. QC carried out bioinformatic  
420 analyses. SWM, EM, and AZ constructed mutants and measured their activity. SWM and ALS  
421 developed and conducted radioassays. SWM together with QC, ALS, EPG, and DB interpreted data and  
422 wrote the manuscript.

423 **Competing interests**

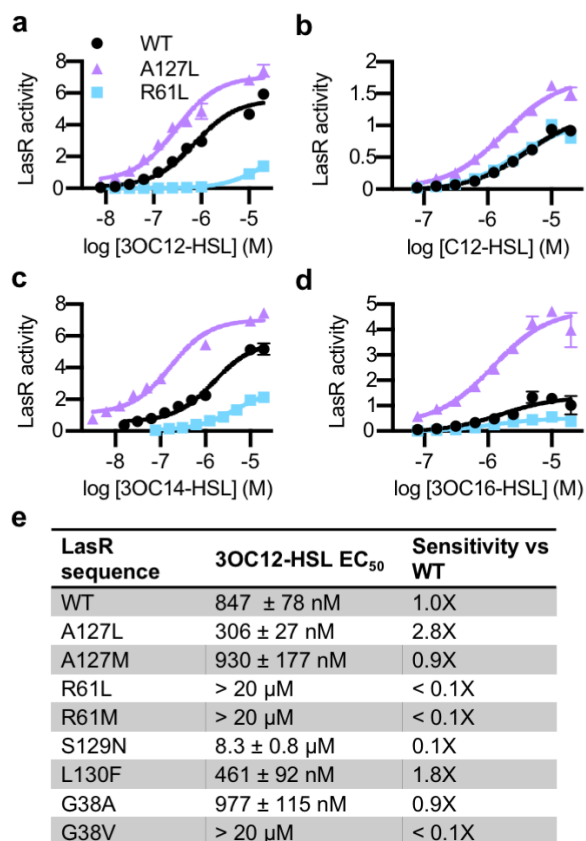
424 The authors declare no competing interests.





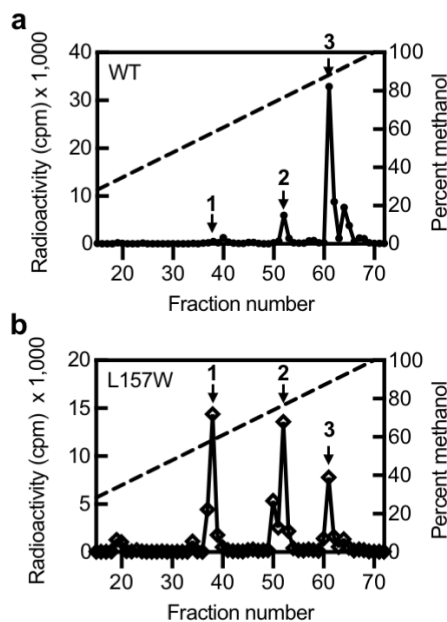
435

436 **Fig. 2 | Covarying residues identified in LasI/R.** **a)** Top-scoring covarying residues in LasI (synthase)  
 437 and LasR (receptor) along with the top GREMLIN score (with APC) for each residue pair based an  
 438 integrated analysis of the Las and Lux systems. **b)** Top-scoring residues in a randomized control,  
 439 mapped onto LasI/R, along with the GREMLIN score (with APC) for each pair. **c)** Top-scoring  
 440 covarying residues mapped onto LasR (covarying residues in orange, 3OC12-HSL in silver; PDB 3IX3)  
 441 and **e)** LasI (covarying residues in blue; PDB 1RO5). Top-scoring residues in the randomized control are  
 442 mapped onto **d)** LasR and **f)** LasI as in panels **c** and **e**.



443

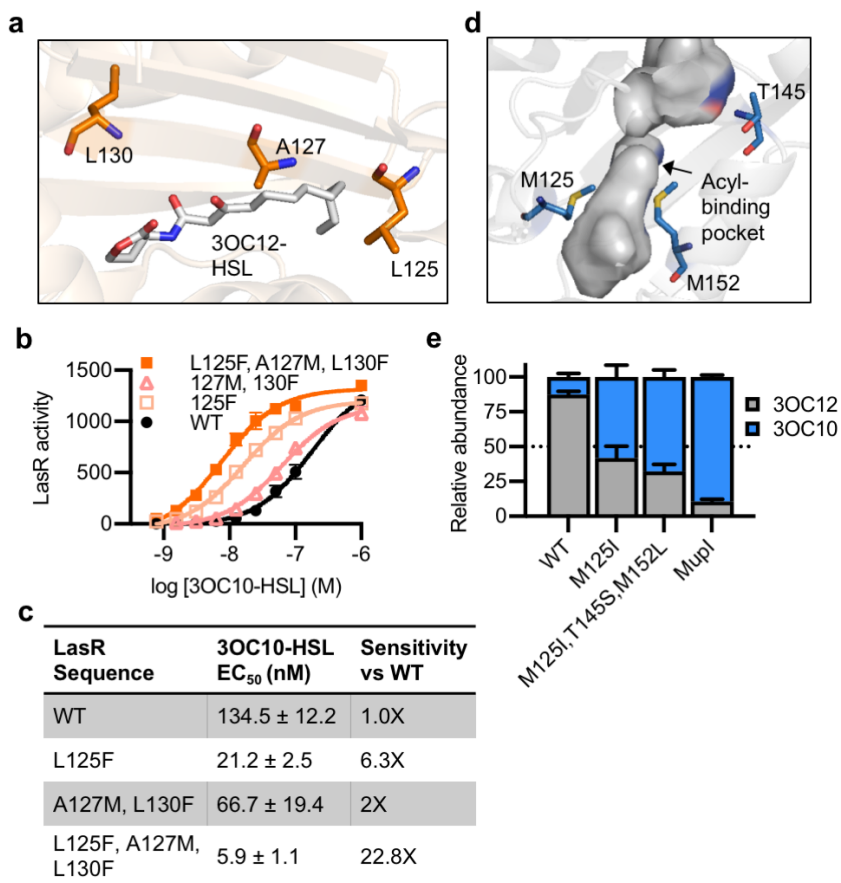
444 **Fig. 3 | Activity of LasR mutants.** Activity of chromosomal *lasR* mutants in *P. aeruginosa* PAO-SC4  
 445 pPROBE-P<sub>rsaL</sub> in response to **a**) 3OC12-HSL, **b**) *N*-dodecanoyl-L-homoserine lactone (C12-HSL), **c**) *N*-  
 446 3-oxo-tetradecanoyl-L-homoserine lactone (3OC14-HSL) or **d**) *N*-3-oxo-hexadecanoyl-L-homoserine  
 447 lactone (3OC16-HSL). Indicated mutations are amino acid substitutions. Wild-type (WT) is shown in  
 448 black, LasR<sup>A127L</sup> in purple, and LasR<sup>R61L</sup> in blue. The horizontal axis indicates AHL concentration. LasR  
 449 activity is reported on the vertical axis as relative fluorescence units normalized by optical density at 600  
 450 nm (RFU/OD x 1,000). Data are the mean and standard deviation of three biological replicates and are  
 451 representative of three independent experiments. **e**) Concentration for half-maximal activation (EC<sub>50</sub>) of  
 452 3OC12-HSL for *P. aeruginosa* PAO-SC4 LasR mutants calculated from data in Supplementary Fig. 3.  
 453 Data are the mean and SEM of three (mutants) or four (wild-type) independent experiments. Sensitivity  
 454 of the mutants compared to LasR<sup>WT</sup> is calculated by dividing WT EC<sub>50</sub> by mutant EC<sub>50</sub>.



455

456 **Fig. 4 | Activity of LasI mutants.** HPLC analysis of radiolabeled AHLs extracted from *P. aeruginosa*  
457 PAO-SC4 harboring a) pJN-RBSlasI<sup>WT</sup> or b) pJN-RBSlasI<sup>L157W</sup>. The horizontal axis denotes the HPLC  
458 fraction number (fractions 1-14 are not shown). The methanol gradient is indicated as a dashed line  
459 plotted on the right vertical axis. The left vertical axis indicates the amount of radioactivity (counts per  
460 minute (cpm)) in each fraction. Data are representative of two (L157W) or three (WT) independent  
461 experiments. Arrow 1 indicates the fraction in which 3OC8-HSL elutes, arrow 2 indicates the fraction in  
462 which 3OC10-HSL elutes, and arrow 3 indicates the fraction in which 3OC12-HSL elutes.





463

464 **Fig. 5 | Reprogramming LasI/R selectivity. a)** Residues mutated in LasR shown as orange sticks in the

465 LasR structure (PDB 3IX3). 3OC12-HSL is shown in grey. **b)** LasR activity in response to 3OC10-HSL

466 measured in *E. coli* harboring pJNL (wild-type, WT, or with indicated mutations) and pPROBE-P<sub>rsaL</sub>.

467 Data are the mean and standard deviation of three biological replicates and are representative of three

468 independent experiments. **c)** Concentration of half maximal activity (EC<sub>50</sub>) of 3OC10-HSL for LasR,

469 calculated from data shown in panel **b**. Data are mean and SEM. Sensitivity of mutants compared to

470 LasR<sup>WT</sup> is calculated by dividing the WT EC<sub>50</sub> by mutant EC<sub>50</sub>. **d)** Residues mutated in LasI shown as

471 blue sticks in the LasI structure (PDB 1ROH). **e)** Relative amount of AHLs produced by *P. aeruginosa*

472 PAO-SC4 harboring pJN-RBS<sub>lasI</sub> (WT or with the indicated mutations) or pJN-RBS<sub>mupI</sub>. Ratios were

473 calculated from HPLC data shown in Supplementary Fig. 6. Bars show mean and standard deviation.

474 The dashed line indicates equal production of 3OC10-HSL and 3OC12-HSL.